4-2006

Thermal Stability and Degradation Kinetics of Poly(methyl Methacrylate)/Layered Copper Hydroxy Methacrylate Composites

Everson Kandare
Marquette University

Hongmei Deng
Marquette University

Dongyan Wang
Cornell University

Jeanne Hossenlopp
Marquette University, jeanne.hossenlopp@marquette.edu

Thermal Stability and Degradation Kinetics of Poly(methyl Methacrylate)/Layered Copper Hydroxy Methacrylate Composites

Everson Kandare

Department of Chemistry, Marquette University
Milwaukee, WI

Hongmei Deng

Department of Chemistry, Marquette University
Milwaukee, WI

Dongyan Wang

Department of Materials Science and Engineering, Cornell University
416 Bard Hall, Ithaca, NY

Jeanne M. Hossenlopp

Department of Chemistry, Marquette University
Milwaukee, WI

Abstract:

Poly(methyl methacrylate) (PMMA)/copper hydroxy methacrylate (CHM) composites were prepared via solution blending and bulk polymerization. Addition of 3% by weight of the CHM additive using solution blending resulted in a significant increment ($\sim$45°C) in thermogravimetric

analysis (TGA) T_{50}, the temperature at which 50% of the original polymeric mass is lost. The value T_{50} increased by 30°C for a PMMA composite with 4% CHM, synthesized via bulk polymerization. Activation energies, E_a, were calculated as a function of conversion fractions (TGA decomposition profile) for the polymeric materials. Analysis of multiple heating rate data using the Flynn–Wall–Ozawa method resulted in E_a values that were 50 kJ mol^{-1} higher for conversions above 0.5 in the solution blended composite compared to a reference sample of pure PMMA recrystallized from the same solvent. Similar results were obtained for bulk polymerization process with differences in E_a values > 30 kJ mol^{-1} relative to pure PMMA. However, in contrast to previous studies of bulk polymerized samples, the solution-blended composite exhibited no improvement in cone calorimetry determination of total heat release as compared with the reference PMMA sample

Keywords: poly(methyl methacrylate), layered hydroxy salt, degradation, thermogravimetric analysis (TGA), composites.

Introduction

Inorganic/organic hybrid layered materials with nanodimensional interlayer spacings can form nanocomposites with polymers either via intercalation or exfoliation.[1–7] Marked improvements, relative to the pure polymer, have been reported in physical properties of these nanocomposites including the tensile strength, tensile modulus, flexural strength, thermal, and corrosion stability compared to virgin polymers.[8–15] In addition to natural cationic clays, synthetic anion clays such as layered double hydroxides and hydroxy double salts (HDSs) have been utilized for this purpose.[16] HDSs are formed from two divalent metals and have the general formula $[M^{2+}_{1-x}M'^{2+}_{1+x}(OH)_{3(1-y)/n}]^+ A^{n-}_{(1+3y)/n} \cdot mH_2O$, where M^{2+}and M'$^{2+}$ represent the different divalent metals and A^{n-}-represents the interlayer anions. Similarly, layered hydroxy salts (LHSs), with a general formula, $M_2(OH)_3(An) \cdot zH_2O$, consist of positively charged metal hydroxide layers and exchangeable interlayer anions, . The advantage of synthetic "clays" is the possibility of varying the identity and composition of constituent metal elements hence providing additional design parameters to optimize additive effects on the properties of the virgin polymer.

Thermal degradation patterns of poly(methyl methacrylate) (PMMA) and PMMA-clay nanocomposites have been extensively

studied.[17–20] Addition of copper-containing layered hydroxides to PMMA through bulk polymerization has been shown in previous work to result in a dramatic improvement in the thermal stability of the resultant composites.[21] In particular, a significant reduction in the total heat release (THR) (~20–30%) from combustion of the composites was observed using cone calorimetry for these microcomposites. However, the need to improve the HDS or LHS additive dispersion was noted and further work was needed to investigate the details of how the additives serve to enhance PMMA thermal stability.[21] Nanoscale dispersion of the additives in the polymer matrix results in a large interfacial area between the polymer chains and the additive leading to physical property enhancements observed for polymer nanocomposites. In clay nanocomposites, typically nanodispersion occurs via intercalation and exfoliation. However, nanocomposites may be more broadly defined, as the dispersion of nano-sized particles in the polymer matrix, thus leading to polymer/additive interaction at the nanoscale. For example polymer nanocomposites containing metal, silica or metal oxide nanoparticles have been shown to exhibit enhanced mechanical, magnetic, optical, or electrical properties.[8,12,15,22–24]

In the work reported here, a LHS additive, copper hydroxy methacrylate (CHM) is added to PMMA via solution blending and bulk polymerization. Composites are analyzed using X-ray diffraction (XRD), transmission electron microscopy (TEM), and Fourier transform infrared (FT-IR) spectroscopy. The effects of sample preparation method on the composite thermal stability are determined via thermogravimetric analysis (TGA), differential thermal analysis (DTA), and cone calorimetry. XRD analysis is used to follow the evolution of the copper content of the additive during heating in order to explore the potential roles that the metal may play in thermal stabilization of PMMA.

Kinetics studies of the thermal degradation of PMMA and its composites have also been shown to be helpful for analyzing thermal stabilization effects.[25–31] In the work reported here, activation energies are determined via an isoconversional method over the range of mass-loss conversions (a) in multiple-heating-rate TGA experiments.

Experimental

Monomeric methyl methacrylate (MMA), benzoyl peroxide (BPO) initiator, reagent grade acetone, NaOH, and commercial PMMA (molecular weight of 996,000 g mol^{-1}) were obtained from Aldrich Chemical Co. Copper(II) methacrylate hydrate (97%) [(H$_2$C=C(CH$_3$)CO$_2$)$_2$Cu · xH$_2$O] and FT-IR-grade KBr were obtained from Alfar Aesar. All chemicals were used without further purification with the exception of the MMA solution where the hydroquinone mono methyl ether inhibitor was removed by passing through an inhibitor removal column (Aldrich).

The LHS additive, CHM, was prepared via a standard literature method used for the preparation of isomorphic LHSs like Cu$_2$(OH)$_3$(CH$_3$CO$_2$) · xH$_2$O.[32] NaOH (0.1 M; 500 ml) was added in a dropwise fashion to 500 ml of 0.1 M copper(II) methacrylate hydrate yielding a pH of 8.1 ± 0.1. The dispersion was filtered, washed, and dried at room temperature.

A 3% loaded PMMA/layered CHM (PMMA/CHM-3) composite was made via solution blending by mixing 97 g of the commercial PMMA, dissolved in 800 ml of acetone for 3 hr, with 3 g of CHM which had been dispersed in 200 ml of acetone for 1 hr. The resultant mixture was mechanically stirred for 96 hr. The resulting viscous liquid was poured out onto an aluminum foil boat to maximize the evaporation of acetone. The composite was then oven dried at 100°C for 6 hr after which it was crushed and dried again until a constant mass was achieved. A reference sample was made from dissolving 100 g of commercial PMMA in 1 l of acetone then allowing the solvent to evaporate. This sample, (PMMA/ CHM-0) was cured in the same way as PMMA/CHM-3.

A 4% CHM loaded PMMA composite (PMMA/CHM-4B) was synthesized via bulk polymerization as described previously.[21] MMA monomer was introduced into a 200 ml beaker together with the initiator, BPO (1%), and the CHM additive. The mixture was initially heated to 90°C with vigorous stirring until viscous after which the temperature was then lowered to 60°C and held constant for 24 hr. The temperature was then raised to 80°C and held at that temperature for another 24 hr followed by drying the sample at 100°C for 12 hr to

drive off excess monomer. Pure PMMA was made in a similar fashion without the additive.

Powder X-ray diffraction (PXRD) patterns of the synthesized layered materials were obtained from a 2θ circle Rikagu diffractometer using Cu-K$_\alpha$ (λ = 1.54 Å) radiation source operated at 50 kV and 20 mA, with data acquisition done in 2θ steps of 0.036° per 20 sec. Powdered samples were mounted on quartz slides using 10% (v/v) GE 7031 epoxy in ethanol after it was found that the mounting process did not perturb the XRD patterns. Polymer composite samples were pressed into 1 mm thick platelets, which were then mounted onto vertically oriented sample holders for XRD analysis. Basal spacing of the synthesized clays and polymer composites were obtained from 00*l* (*l* = 1–3) reflections after fitting the raw spectra to a pseudo-Voight XFIT[33] program, stripping off the Cu-K$_{\alpha 2}$ contribution. Average crystallite sizes, τ, were determined using the Debye–Scherrer equation:

$$\tau = \kappa\lambda/(\beta_\tau \cos\theta)$$

(1)

Where κ is a constant (0.9 for powders),[34] β_τ is the full width at half-maximum height of the target diffraction peak of the material after correction for Cu-K$_{\alpha 2}$ and the instrumental broadening, and λ is the X-ray wavelength, 1.54 Å for Cu-K$_{\alpha 1}$.

FT-IR spectra of the composites were determined using the KBr method on a Nicolet Magna-IR 560 spectrometer. FT-IR spectra were acquired at 1 cm^{-1} resolution, in the 400–4000 cm^{-1} region, averaging 40 scans. TGA and DTA were performed on a SDT 2960 simultaneous DTA–TGA instrument from 50 to 600°C using constant heating rates of 10, 15, 20, and 25 K/min in air, flowing at 85 ± 5 ml min^{-1}, with sample sizes of 21.0 ± 1.0 mg contained in aluminum cups. A Mattson–Cahn TG–131-TGA coupled to a FT-IR (TGA-FTIR) instrument was employed in this study to monitor the gases evolved during combustion processes. TGA-FTIR experiments were performed on 50 ± 5 mg samples that were heated between 50 and 600°C at 20°C min^{-1} with air as the purge gas (flow rate, 85 ± 5 ml min^{-1}).

PMMA composite samples (30g) were compression molded into 10 cmx10 cm square plaques of uniform thickness (~2 mm) before cone calorimetry was performed on an Atlas Cone 2 instrument, incident flux of 35 kW m^{-2}. Bright field TEM images were collected at 60 kV with a Zeiss 10c electron microscope at Cornell University.

Results and Discussion

The PXRD pattern of the CHM additive, $Cu_2(OH)_3$ $(H_2C=C(CH_3)CO_2) \cdot zH^2O$, is shown in trace (a) in Fig. 1(A). The XRD data exhibit similar features to isomorphic $Cu2(OH)3(CH3CO2) \cdot zH2O$ which has been reported to have a botallackite-type structure.[35] Using Bragg's equation, $\lambda = 2d\sin\theta$, and the 001 reflection, the basal spacing, d, is found to be 11.5 Å. No significant change in the d spacing was observed for PMMA/CHM-4B made through bulk polymerization as shown in Fig. 1(A). The XRD patterns of CHM and PMMA/CHM-3, obtained on a different X-ray diffractometer (Cornell University), are shown in Fig. 1(B). After solution blending of the model compound, CHM, with PMMA in acetone, the basal spacing increased to 12.8 Å indicating that the structure has been swelled as a result of sample preparation, suggesting some minor intercalation.

XRD alone cannot sufficiently characterize the nature of the dispersion of the additive in PMMA. TEM was employed to examine the microstructure of the PMMA/CHM-3 composite. TEM provides information about spatial distribution of the additive in a local area of the composite. Figure 2 shows TEM images for the PMMA/CHM-3 sample at both low and high magnification. The low magnification TEM image shows that CHM is fairly well distributed. Dark lines running approximately parallel to each other are clearly seen in the low magnification image. The average thickness of these dark lines is 458 ± 7 Å corresponding to 36 ± 1 layers of the copper hydroxyl sheets stacked upon each other taking the basal spacing to be 12.8 Å as calculated for PMMA/CHM-3. The crystallite size of CHM in the *c*-axis direction was calculated independently using the Debye-Scherrer equation to be 390 ± 25 Å corresponding to 34 ± 3 copper hydroxide layers stacked together. These data suggest that some of the CHM phase remains intact during polymerization. While the 001 peak in the PMMA/CHM-3 composite is narrower than for CHM itself, this effect cannot be attributed to particle size increase since mixed-layering and

preferred orientations are known to perturb XRD measurements in organo-clay dispersions.[36]

The high magnification TEM image is consistent with neither delamination nor exfoliation. Nanoscale tactoids are observed but there is not enough evidence to suggest intercalation. This is consistent with a small increase in *d* spacing from XRD, which suggest no meaningful intercalation. Even though XRD patterns and TEM images do not give conclusive evidence of nanocomposite formation via the routes typically observed for polymer/clay samples, the presence of nanometric crystallite sizes of CHM in at least one dimension suffices to describe PMMA/CHM-3 as a nanocomposite.

TGA curves showing the variation of undecomposed mass percentage as a function of temperature for pure PMMA, PMMA/CHM-0, and PMMA/CHM-3 are presented in Fig. 3(A). The thermal degradation of pure PMMA prepared by free radical polymerization is expected to show three stages of mass loss.[26,37–39] The first stage of thermal degradation is initiated by scission of weak peroxide and hydroperoxide linkages mainly due to the combination of monomer with O_2 during synthesis.[40] Head-to-head (H–H) linkages from termination by combination are also easily broken at relatively low temperatures, leading to the production of free radicals, which will participate in the further depolymerization at higher temperatures through chain transfer processes. The second weight loss is largely a result of scission at the unsaturated ends due to termination by disproportionation. This process involves homolytic cleavage of the C–C bond β to the vinyl group while the last step is mainly due to the random chain scission of the PMMA backbone.[38]

From Fig. 3(A), commercial PMMA shows no weight loss at low temperatures (<250°C) as is also evident in the corresponding derivatized thermal gravimetric analysis (DTG) plot of $\delta\alpha/\delta T$ versus temperature shown in Fig. 3(B). However, multiple overlapping weight losses are observed from approximately 250°C to 440°C for pure PMMA. This is consistent with a previous report of TGA of commercial PMMA with the same molecular weight.[26] In contrast, for the recrystallized sample (PMMA/CHM-0), a significant (~10%) mass loss occurs at a lower temperature as compared to the commercial sample. TGA-FTIR analysis confirms that this is due to the loss of acetone, the

solvent used to prepare solution-blended samples. The first stage of weight loss for PMMA/CHM-3, begins at about 150°C and corresponds to the loss of the water and methacrylate from the additive as well as residual acetone. However, the remainder of the degradation pattern for PMMA/CHM-3 is significantly shifted to higher temperatures (see Fig. 3A and 3B) suggesting that the polymeric composite is more thermally stable than the commercial PMMA and the PMMA/CHM-0 sample.

From Fig. 3(A), the temperatures at which 10, 50, and 90% mass of the polymer composite are lost, T_{10}, T_{50}, T_{90} are 33, 45, and 20°C higher for PMMA/CHM-3 than for PMMA/ CHM-0 respectively. Chen and coworkers reported a positive shift of 45°C in the T_{50} value by modifying PMMA with 30 wt% MgAl (dodecyl sulfate), a layered double hydroxide.[41] However, such high loadings can significantly affect the mechanical properties of the composites in an undesirable way. The significant improvement in the threshold temperatures of PMMA/CHM-3 at 3% loading is promising for development of this new class of additives.

Figure 4(A) shows TGA curves for pure PMMA and PMMA/CHM-4B synthesized via bulk polymerization, with corresponding DTG plots provided in Fig. 4(B). Three stages of thermal decomposition are clearly seen for pure PMMA. The first stage in mass loss at about 200°C should correspond to depolymerization initiated by weak H–H linkages together with weak peroxides and/or hydroperoxides linkages.[40] However, this stage is insignificant, suggesting that there are few of the above-mentioned linkages. The second stage at about 300°C is a result of radical transfer to unsaturated chain ends while the last stage around 365°C corresponds to random scission.[38] PMMA/CHM-4B shows a similar behavior except that the degradation temperatures at maximum weight loss for the three stages are shifted to higher values, implying improved thermal stability. The second and last stages of mass losses for pure PMMA in the DTG plots are substantial and equally important while for PMMA/CHM-4B the second mass loss (~300°C) is less pronounced than the last stage, which is also shifted to higher temperatures, (~390°C) relative to pure PMMA.

Figure 5(A) shows DTA curves for pure PMMA, PMMA/ CHM-0, and PMMA/CHM-3 composite. The DTA curves are shown to draw a

comparison between thermal degradation behaviors of pure PMMA and PMMA/CHM-0 to that of the polymer composite, PMMA/CHM-3. The DTA curves for pure PMMA and PMMA/CHM-0 show similar behavior throughout the decomposition process. Three endotherms are seen around 270, 330, and 380°C while one exotherm is observed at about 420°C. In contrast, the PMMA/CHM-3 composite shows an exotherm around 280°C (possibly due to oxidation of organic interlayer species) followed by an endotherm at about 330°C similar to the reference samples.

The second endothermic process for PMMA/CHM-3 occurs at a slightly higher temperature, 390°C, as compared to about 380°C for the reference samples consistent with improved thermal stability of the composite. The last exothermic process for the composite is slightly shifted to a higher temperature but is of similar magnitude to pure PMMA, and PMMA/CHM-0. This suggests that the mass losses at higher conversion fractions in both the reference materials and the composite are due to the same basic mechanism.

Figure 5(B) shows DTA curves for pure PMMA and PMMA/CHM-4B composite synthesized via bulk polymerization. The DTA curve for pure PMMA shows two overlapping endotherms starting at 250 to 420°C and a small exothermic feature at 430°C. However, three endotherms are seen at around 265, 300, and 400°C for PMMA/CHM-4B. An exotherm at around 250°C is due to the thermal degradation of interlayer organic species contained in the additive. An exothermic process at 430°C in the PMMA/CHM-4B sample is enhanced relative to that observed for the pure PMMA. This suggests that a significant mass loss occurs at elevated temperatures for the composite material, mainly due to random chain scission. The notable difference in the DTA curves for pure PMMA and PMMA/CHM-4B might suggest a change in the relative contribution of the different degradation processes for these polymeric materials. Further work is required to test this hypothesis.

Thermogravimetric measurements provide a qualitative means of estimating the thermal stability of polymeric materials.[42,43] Thermal stability is defined here as the onset temperature for degradation and the rate of degradation of the respective materials. As noted earlier, the thermal degradation of PMMA and PMMA/CHM composites involves

multiple degradation steps. A simple means of extracting effective kinetic parameters from these rather complicated decomposition processes is analysis of multiple heating rate kinetics (MHRKs), applying the commonly used Flynn–Wall–Ozawa[44,45] method specifically derived for heterogeneous chemical reactions under linear heating rates. The Flynn-Wall-Ozawa method is expressed by the equation:

$$\log f(x) = \log\left(\frac{AE_a}{R}\right) - \log(\beta) - 2.315 - \frac{0.456E_a}{RT} \qquad (2)$$

Where $f(x)$ is known as the conversional functional relationship; *A* is the pre-exponential factor (in min^{-1}), E_a is the apparent activation energy (in kJ mol^{-1}), *R* is the gas constant, β is the heating rate (in K min-1), and *T* is the absolute temperature (in K).

The E_a values for the virgin PMMA, PMMA/CHM-0, PMMA/CHM-3, bulk polymerized pure PMMA, and PMMA/CHM-4B were calculated from slopes of the isoconversional plots of log (β) versus 1/*T*. The E_a values were calculated for fractional conversions α = 0.05 - 0.90 at intervals of 0.05. These values are plotted in Fig. 6(A) and 6(B). The value for the pure commercial PMMA, as received, decreased from 160 to 110 kJ mol^{-1} between and 0.55. The value then increased in a parabolic fashion to a value of 180 kJ mol^{-1} at α = 0.9. Laachachi *et al*. reported similar results for the thermal degradation of PMMA in air.[37] The observed apparent E_a value for the PMMA/CHM-3 increased with conversion to reach a constant E_a value of ~187 kJ mol^{-1} from until the end of the reaction. For decomposition via a single step, the MHRKs are expected to result in constant values as a function of α[45]. Multistep processes, such as those observed here, may result in variations in E_a values over the conversion range, however, unambiguous interpretation of such changes is difficult. There is no significant difference, within experimental error, between the E_a value for PMMA/CHM-0, and PMMA/CHM-3 in the region, α = 0.05 to 0.40. Both samples show higher E_a values than the commercial sample at low temperatures/conversions. However, the complicated nature of mass loss at the earlier degradation stages, particularly in the solution blended samples where solvent loss is occurring, precludes attributing E_a differences at low conversions to significant changes in polymer

stability without additional experimental characterization of degradation products.

A difference of >50 kJ mol^{-1} between the E_a value of PMMA/CHM-0 and PMMA/CHM-3, (α = 0.5 – 0.9) is, however, consistent with the suggestion that the thermal stability of PMMA is greatly enhanced by addition of the LHS, CHM. Similar trends in the E_a values are seen for the samples prepared via bulk polymerization. In contrast to results obtained through solution blending, the E_a values at specific fractional conversions, α, is always higher for PMMA/CHM4B than for pure PMMA. Differences of >30 kJ mol^{-1} in for PMMA/CHM-4B relative to pure PMMA are seen for α = 0.55 – 0.9. However, the general shapes of E_a curves as a function of α are similar for the two preparative methods, suggesting that there is no significant change in the degradation mechanism of composites made from solution blending as compared to those made via bulk polymerization. In both cases the elevated E_a values correlate, as expected, with the observed improved thermal stability of the polymer composites seen in TGA profiles acquired at a single heating rate.

The positive shift in maximum mass-loss temperature for PMMA/CHM-3 implies that the presence of the LHS in the polymer matrix severely limits or prevents depolymerization processes by radical chain transfer (second stage). A greater portion of the polymer composite is then lost through random scission occurring at elevated temperatures. This might be as a result of the formation of organic/ inorganic networks, such as Cu salt ionomers that are thermally more stable than PMMA.[46] In addition these networks may serve to prevent the rapid diffusion of free radicals, which are known to promote the depolymerization process.[47] Also, the presence of the inorganic moieties may serve to stabilize or even trap free radicals by participation in redox reactions as previously hypothesized in the authors' laboratory with HDS and LHS/PMMA composites.[21]

In previous work,[21] differences in copper oxidation states in cone residues were observed for composites made with CHM and a zinc/copper methracrylate HDS. In order to further explore the evolution of copper oxidation states, the PMMA-CHM-4B and pure CHM were heated for TGA at 20°C min^{-1} and the resulting residues were analyzed via XRD. The presence of Cu(I) oxide (PDF# 35-1091)[48] in

the residue of PMMA/CHM-4B after heating to 250°C is observed in the XRD pattern shown in trace (c) of Fig. 1(A). Cu(I) oxide and Cu metal (PDF# 4-836)[48] were seen in the XRD pattern of the pure CHM residue after heating to 270°C. The absence of metallic Cu in the residue of PMMA/CHM-4B at similar temperature suggests that the products of degradation of PMMA may participate in redox reactions with the additive.

Cu(II), in the form of $CuCl_2$, has been reported[49] to have a stabilizing effect on the thermal degradation of PMMA, while Cu(I) (CuCl) did not have any effect on the thermal degradation of PMMA in air. However, several authors have shown that Cu(I) based catalysts can be used in the polymerization of PMMA through atom transfer radical polymerization (ATRP) with high efficiency.[50–52] The presence of Cu(I) ions at temperatures as low as 250°C could establish conditions suitable for living polymerization through radical, MMA · , combination. This could lead to retardation of the depolymerization process as more polymer chains are generated concomitant with the combustion of the starting material. Therefore, the presence of Cu ions in the polymeric matrix during combustion may serve to stabilize the composite materials, consistent with the enhanced TGA residue reported previously for CHM additives with PMMA.[21] Analysis of PMMA/CHM residues to test this hypothesis will be the subject of future work.

The potential effect of additive on the extent of initial polymerization during sample preparation must also be considered, particularly for the bulk polymerized samples. Kashiwagi *et al.*[38] have suggested that a difference in the molecular weights of polymers synthesized via bulk polymerization will affect their degradation profiles. The presence of a Cu(II)-based additive in PMMA/CHM-4B could have an effect on its average molecular weight as compared to pure PMMA. Polymers with fewer unsaturated chain ends would lose less mass in the second degradation stage. To rule out the possibility of having significantly different molecular weights in pure PMMA compared to PMMA/CHM-4B FT-IR analysis was performed for the bulk polymerized samples and the results are presented in Fig. 7. As reported by Suske *et al.*,[53] comparison of the integrated intensities of the C–H stretching bands at about 3000 cm^{-1} to the C=O anti-symmetric stretch at around 1730 cm^{-1} can be used to estimate the extent of crosslinking in PMMA. More highly crosslinked samples have

lower C-H/C=O ratios. Based on the data shown in Fig. 7, the C-H/C=O ratios were found to be 0.74 ± 0.06 and 0.78 ± 0.06 for PMMA and PMMA/CHM-4B respectively, suggesting that there is no significant difference in crosslinking due to the presence of the CHM additive.

Cone calorimetry experiments were performed to investigate the relative flammability of PMMA/CHM-0 to PMMA/CHM-3. Figure 8 shows the variation of heat released with combustion time for the commercial PMMA, PMMA/CHM-0, and PMMA/CHM-3. The THR as depicted by the integrated areas under the respective heat release rate versus time curves are 82.2 ± 2.2, 72.6 ± 0.7, and 71.5 ± 17 MJ m^{-2} for the commercial PMMA, PMMA/CHM-0, and PMMA/CHM-3 respectively. Even though there is a significant reduction in the THR for the recrystallized polymer composites relative to the commercial PMMA, there is, however, no meaningful difference between PMMA/CHM-0 and PMMA/CHM-3.

The obtained kinetic information (activation energies) used to estimate the thermal stability of these polymeric materials is derived from weight loss profiles of thermal degradation processes. The mathematical function used to describe the degradation process is modeled for the released products, i.e., from weight loss, and provides no information about which, or how many bonds are broken at any given conversion fraction.[54] The extracted effective E_a values are thus useful here to explain the shift to higher threshold temperatures for PMMA/CHM-3 but not necessarily its flammability. While TGA curves and apparent E_a values suggest a significant improvement in the thermal stability of PMMA/CHM-3 relative to PMMA/CHM-0, cone calorimetry measurements suggest no difference in their flammability.

Conclusions

CHM has been used as an additive to provide thermal stability to PMMA. Solution blending and bulk polymerization in the presence of 3-4% by mass of the additive result in a significant shift in the temperature for 50% mass loss. Apparent E_a values were significantly higher for the PMMA/CHM-3 composite a difference >50 kJ mol^{-1}) for the later stages of the thermal decomposition process (α = 0.5 – 0.9) compared to the reference sample PMMA/CHM-0. A similar trend was observed for PMMA/CHM-4B with values for the composite being 30 kJ

mol^{-1} greater than the pure PMMA in the region $\alpha = 0.55 - 0.9$. However, in contrast to bulk polymerized samples, no significant difference was observed in the THR in cone calorimetry measurements for the solution blended composite, PMMA/CHM-3, relative to PMMA/CHM-0.

Acknowledgments

References

1. Huang X, Brittain WJ. Synthesis and characterization of PMMA nanocomposites by suspension and emulsion polymerization. *Macromolecules* 2001; 34: 3255–3260.

2. Qu X, Guan T, Liu G, She Q, Zhang L. Preparation, structural characterization, and properties of poly(methyl methacrylate)/montmorillonite nanocomposites by bulk polymerization. *J. Appl. Polym. Sci*. 2005; 97: 348–357.

3. Hwu JM, Jiang GJ, Gao ZM, Xie W, Pan WP. The characterization of organic modified clay and clay-filled PMMA nanocomposite. *J. Appl. Polym. Sci*. 2002; 83: 1702–1710.

4. Yang F, Nelson GL. PMMA/silica nanocomposite studies: synthesis and properties. *J. Appl. Polym. Sci*. 2004; 91: 3844– 3850.

5. Lee DC, Jang LW. Preparation and characterization of PMMA-clay hybrid composite by emulsion polymerization. *J. Appl. Polym. Sci*. 1996; 61: 1117–1122.

6. Shen Z, Simon GP, Cheng Y-B. Nanocomposites of poly(methyl methacrylate) and organically modified layered silicates by melt intercalation. *J. Appl. Polym. Sci.* 2004; 92: 2101–2115.

7. Kumar S, Jog JP, Natarajan U. Preparation and characterization of poly(methyl methacrylate)-clay nanocomposites via melt intercalation: the effect of organoclay on the structure and thermal properties. *J. Appl. Polym. Sci*. 2003; 89: 1186–1194.

8. Aymonier C, Bortzmeyer D, Thomann R, Mulhaupt R. Poly(methyl methacrylate)/palladium nanocomposites: synthesis and

characterization of the morphological, thermomechanical, and thermal properties. *Chem. Mater*. 2003; 15: 4874–4878.

9. Zhu J, Morgan AB, Lamelas FJ, Wilkie CA. Fire properties of polystyrene-clay nanocomposites. *Chem. Mater*. 2001; 13: 3774–3780.

10. Laachachi A, Leroy E, Cochez M, Ferriol M, Lopez Cuesta JM. Use of oxide nanoparticles and organoclays to improve thermal stability and fire retardancy of poly(methyl methacrylate). *Polym. Degrad. Stab*. 2005; 89: 344–352.

11. Bourbigot S, Gilman JW, Wilkie CA. Kinetic analysis of the thermal degradation of polystyrene-montimorillonite nanocomposite. *Polym. Degrad. Stab*. 2004; 84: 483–492.

12. Mallikarjuna NN, Venkataraman A, Aminabhavi TM. A study on γ-Fe$_2$O$_3$ loaded poly(methyl methacrylate) nanocomposites. *J. Appl. Polym. Sci*. 2004; 94: 2551–2554.

13. Yeh J-M, Liou S-J, Lai M-C, Chang Y-W, Huang C-Y, Chen C-P, Jaw J-H, Tsai T-Y, Yu Y-H. Comparative studies of the properties of poly(methyl methacrylate)-clay nanocomposite materials prepared by *in situ* emulsion polymerization and solution dispersion. *J. Appl. Polym. Sci*. 2004; 94: 1936–1946.

14. Yeh J-M, Liou S-J, Lin C-Y, Cheng C-Y, Chang Y-W. Anticorrosively enhanced PMMA-clay nanocomposite materials with quaternary alkylphosphonium salt as an intercalating agent. *Chem. Mater*. 2002; 14: 154–161.

15. Kashiwagi T, Morgan AB, Antonucci JM, VanLandingham MR, Harris RH, Awad WH, Shields JR. Thermal and flammability properties of a silica-poly(methyl methacrylate) nanocomposite. *J. Appl. Polym. Sci.* 2003; 89: 2072–2078.

16. Rajamathi M, Thomas GS, Kamath PV. The many ways of making anionic clays. *Proc. Indian Acad. Sci., Chem. Sci*. 2001; 113: 671–680.

17. Chandrasiri JA, Wilkie CA. Thermal degradation of poly(methyl methacrylate) in the presence of tin(IV) chloride and tetraphenyltin. *Polym. Degrad. Stab*. 1994; 45: 91–96.

18. Wang D, Zhu J, Yao Q, Wilkie CA. A comparison of various methods for the preparation of polystyrene and poly(methyl methacrylate) clay nanocomposites. *Chem. Mater*. 2002; 14: 3837–3843.

19. Du J, Zhu J, Wilkie CA, Wang J. An XPS investigation of thermal degradation and charring on PMMA clay nanocomposites. *Polym. Degrad. Stab*. 2002; 77: 377–381.

20. Su S, Wilkie CA. Exfoliated poly(methyl methacrylate) and polystyrene nanocomposites occur when the clay cation contains a vinyl monomer. *J. Polym. Sci., Part A: Polym. Chem*. 2003; 41: 1124–1135.

21. Kandare E, Hall D, Jiang DD, Hossenlopp JM. Development of new fire retardant additives based on hybrid inorganic/ organic nanodimensional layered compounds: thermal degradation of PMMA composites. *ACS Symposium Series 922, Fire and Polymers IV: Materials and Concepts for Hazard Prevention*. Wilkie CA, Nelson GL (eds), American Chemical Society: Washington, DC, 2006; 131–143.

22. Beecroft LL, Ober CK. Nanocomposite materials for optical applications. *Chem. Mater*. 1997; 9: 1302–1317.

23. Sidorov SN, Volkov LV, Davankov VA, Tsyurupa MP, Valetsky PM, Bronstein LM, Karlinsey R, Zwanziger JW, Matveeva VG, Sulman EM, Lakina NV, Wilder EA, Spontak RJ. Platinum-containing hyper-cross-linked polystyrene as a modifier-free selective catalyst for L-sorbose oxidation. *J. Am. Chem. Soc*. 2001; 123: 10502–10510.

24. Landry CJT, Coltrain BK, Landry MR, Fitzgerald JJ, Long VK. poly(viny1 acetate)/silica filled materials: material properties of *in situ* vs fumed silica particles. *Macromolecules* 1993; 26: 3702–3712.

25. Jellinek HHG, Luh MD. Thermal degradation of isotactic and syndiotactic poly(methyl methacrylate). *J. Phys. Chem*. 1996; 70: 3672–3680.

26. Ferriol M, Gentilhomme A, Cochez M, Oget N, Mieloszynski JL. Thermal degradation of poly(methyl methacrylate) (PMMA): modelling of DTG and TG curves. *Polym. Degrad. Stab*. 2003; 79: 271–281.

27. Gao Z, Kaneko T, Hou D, Nakada M. Kinetics of thermal degradation of poly(methyl methacrylate) studied with the assistance of the fractional conversion at the maximum reaction rate. *Polym. Degrad. Stab*. 2004; 84: 399–403.

28. Hu Y-H, Chen C-Y. The effect of end groups on the thermal degradation of poly(methyl methacrylate). *Polym. Degrad. Stab*. 2003; 82: 81–88.

29. Hu Y-H, Chen C-Y. Study of the thermal behavior of poly(methyl methacrylate) initiated by lactams and thiols. *Polym. Degrad. Stab*. 2003; 80: 1–10.

30. Peterson JD, Vyazovkin S, Wight CA. Kinetic study of stabilizing effect of oxygen on thermal degradation of poly(metyl methacrylate). *J. Phys. Chem*. B. 1999; 103: 8087–8092.

31. Holland BJ, Hay JN. The kinetics and mechanisms of the thermal degradation of poly(methyl methacrylate) studied by thermal analysis-Fourier transform infrared spectroscopy. *Polymer* 2001; 42: 4825–4835.

32. Jimenez-Lopez A, Rodriguez-Castellon E, Olivera-Pastor P, Maireles-Torres P, Tomlinson AAG, Jones DJ, Roziere J. Layered basic copper anion exchangers: chemical characterization and X-ray absorption study. *J. Mater. Chem*. 1993; 3: 303–307.

33. Cheary RW, Coelho AA. Programs XFIT and FOURYA, deposited in CCP14. Powder Diffraction Library, Engineering and Physical Sciences Research Council, Daresbury Laboratory, Warrington. http://www.ccp14.ac.uk/tutorial/xfit-95/xfit.htm 1996.

34. Jenkins R, Synder RL. *Introduction to X-ray Powder Diffractometry*. Wiley: New York, 1996.

35. Yamanaka S, Sako T, Seki K, Hattori M. Anion exchange reactions in layered basic copper salts. *Solid State Ionics* 1992; 53–56: 527–533.

36. Eckel DF, Balogh MP, Fasulo PD, Rodgers WR. Assessing organo-clay dispersion in polymer nanocomposites. *J. Appl. Polym. Sci*. 2004; 93: 1110–1117.

37. Laachachi A, Cochez M, Ferriol M, Leroy E, Lopez Cuesta JM, Oget N. Influence of Sb_2O_3 particles as filler on the thermal stability and flammability properties of poly(methyl methacrylate) (PMMA). *Polym. Degrad. Stab*. 2004; 85: 641–646.

38. Kashiwagi T, Inaba A, Brown JE, Hatada K, Kitayama T, Masuda E. Effects of weak linkages on the thermal and oxidative degradation of poly(methy1 methacrylates). *Macromolecules* 1986; 19: 2160–2168.

39. Laachachi A, Cochez M, Ferriol M, Lopez Cuesta JM, Leroy E. Influence of TiO_2 and Fe_2O_3 fillers on the thermal properties of poly(methyl methacrylate) (PMMA). *Mater. Lett*. 2005; 59: 36–39.

40. Holland BJ, Hay JN. The effect of polymerization conditions on the kinetics and mechanisms of thermal degradation of PMMA. *Polym. Degrad. Stab*. 2002; 77: 435–439.

41. Chen W, Feng L, Qu B. In situ synthesis of poly(methyl methacrylate)/MgAl layered double hydroxide nanocomposite with high
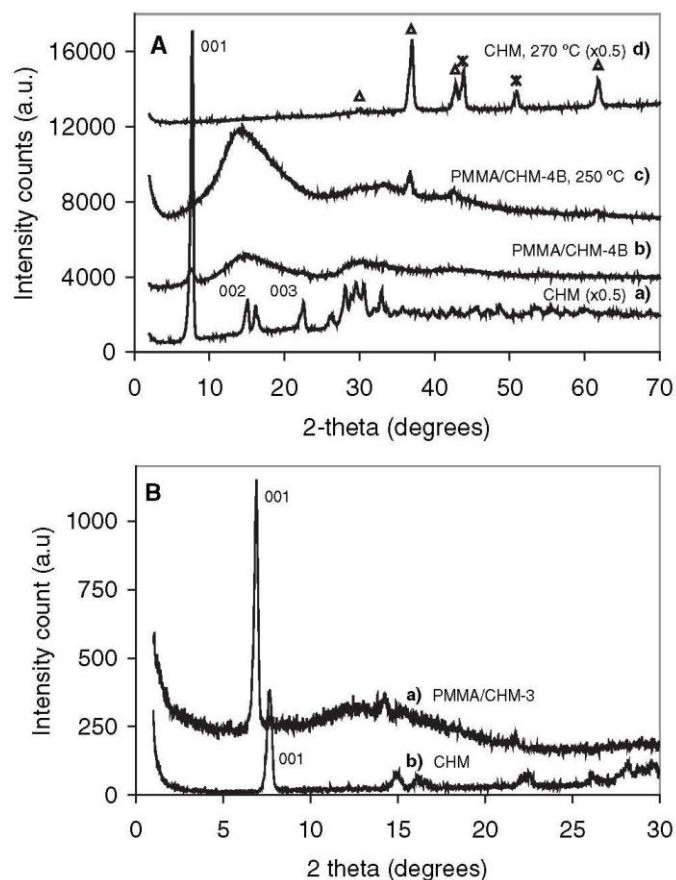
transparency and enhanced thermal properties. *Solid State Commun*. 2004; 130: 259–263.

42. Vyazovkin S, Wight CA. Isothermal and nonisothermal reaction kinetics in solids: in search of ways toward consensus. *J. Phys. Chem*. *A*. 1997; 101: 8279–8284.

43. Khawam A, Flanagan DR. Complementary use of model-free and modelistic methods in the analysis of solid-state kinetics. *J. Phys. Chem*. B. 2005; 109: 10073–10080.

44. Ozawa T. A new method of analyzing thermogravimetric data. *Bull. Chem. Soc.* Jpn 1965; 38: 1881–1886.

45. Vyazovkin S. Evaluation of activation energy of thermally stimulated solid-state reactions under arbitrary variation of temperature. *J. Comp. Chem*. 1997; 18: 393–402.

46. Kosyanchuk LF, Lipatova TE, Vilensky VA, Lipatov YS, Shtompel VI. Polyurethanes crosslinked by metals and their complexes with crown ether. *J. Polym. Sci., Part A: Polym. Chem*. 1998; 36: 1379–1386.

47. Wang H, Xu P, Zhong W, Shen L, Du Q. Transparent poly(methyl methacrylate)/silica/zirconia nanocomposites with excellent thermal stabilities. *Polym. Degrad. Stab*. 2005; 87: 319–327.

48. Powder Diffraction File Alphabetical Indexes. Inorganic Phases. JCPDS, International Centre for Diffraction Data, Swartmore, PA, 1999.

49. Chandrasiri JA, Roberts DE, Wilkie CA. The effect of some transition metal chlorides on the thermal degradation of poly(methyl methacrylate): a study using TGA-FTIR spectrometry. *Polym. Degrad. Stab*. 1994; 45: 97–101.

50. Darcos V, Monge S, Haddleton DM. In situ Fourier transform near infrared spectroscopy monitoring of copper mediated living radical polymerization. *J. Polym. Sci., Part A: Polym. Chem*. 2004; 42: 4933–4940.

51. Miura Y, Satoh T, Narumi A, Nishizawa O, Okamoto Y, Kakuchi T. Atom transfer radical polymerization of methyl methacrylate in fluoroalcohol: simultaneous control of molecular weight and tacticity. *Macromolecules* 2005; 38: 1041–1043.

52. Percec V, Asandei AD, Asgarzadeh F, Bera TK, Barboiu B. Cu^I and Cu^{II} salts of group VIA elements as catalysts for living radical polymerization initiated with sulfonyl chlorides. *J. Polym. Sci., Part A: Polym. Chem*. 2000; 38: 3839–3843.

53. Suske E, Scharf T, Krebs H-U, Panchenko E, Junkers T, Egorov M, Buback M, Kijewski H. Tuning of cross-linking and mechanical properties of laser-deposited poly(methyl methacrylate) films. *J. Appl. Phys*. 2005; 97: 63501–63504.

54. Maciejewski M. Thermal analysis and kinetic concepts of solid-state reactions. *J. Therm. Anal.* 1988; 33: 1269–1277.
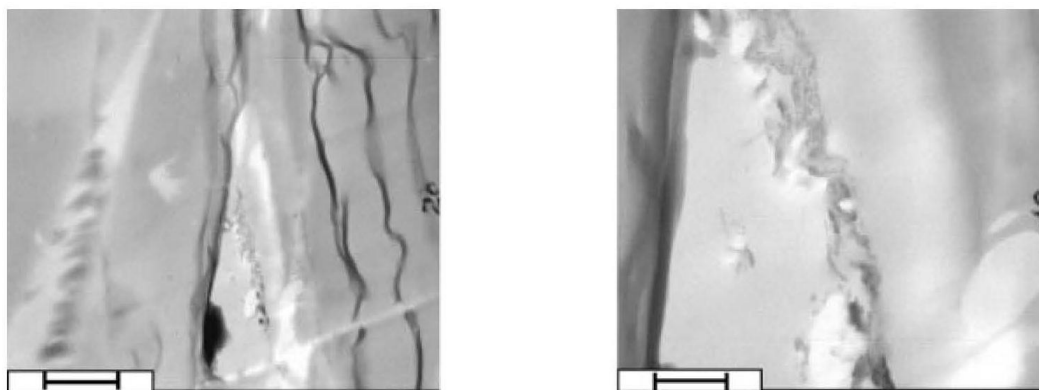
About the Authors

Jeanne M. Hossenlopp : Department of Chemistry, Marquette University, P. O. Box 1881, Milwaukee, WI 53201-1881, USA.

Email : Jeanne.Hossenlopp@marquette.edu

Figure 1

(A) XRD pattern of: (a) additive, CHM (scaled by a factor of 0.5); (b) PMMA/CHM-4B composite; (c) residue after heating PMMA/CHM-4B to 250°C; (d) residue after heating CHM to 270°C at 20°C min-1 (scaled by a factor of 0.5), assignment of CuO (Δ) and Cu^0 (*) reflections is indicated. Data are offset for clarity.
(B) XRD pattern of: (a) PMMA/CHM-3; (b) the additive, CHM. The XRD patterns in Fig. 1(B) were collected at Cornell University using a different instrument than used for patterns in Fig. 1(A).

Figure 2

TEM images at low (left) and high (right) magnification for PMMA/CHM-3. For low magnification, the scale bar (bottom left) represents 500 nm while for high magnification, the scale bar (bottom left) represents 100 nm.
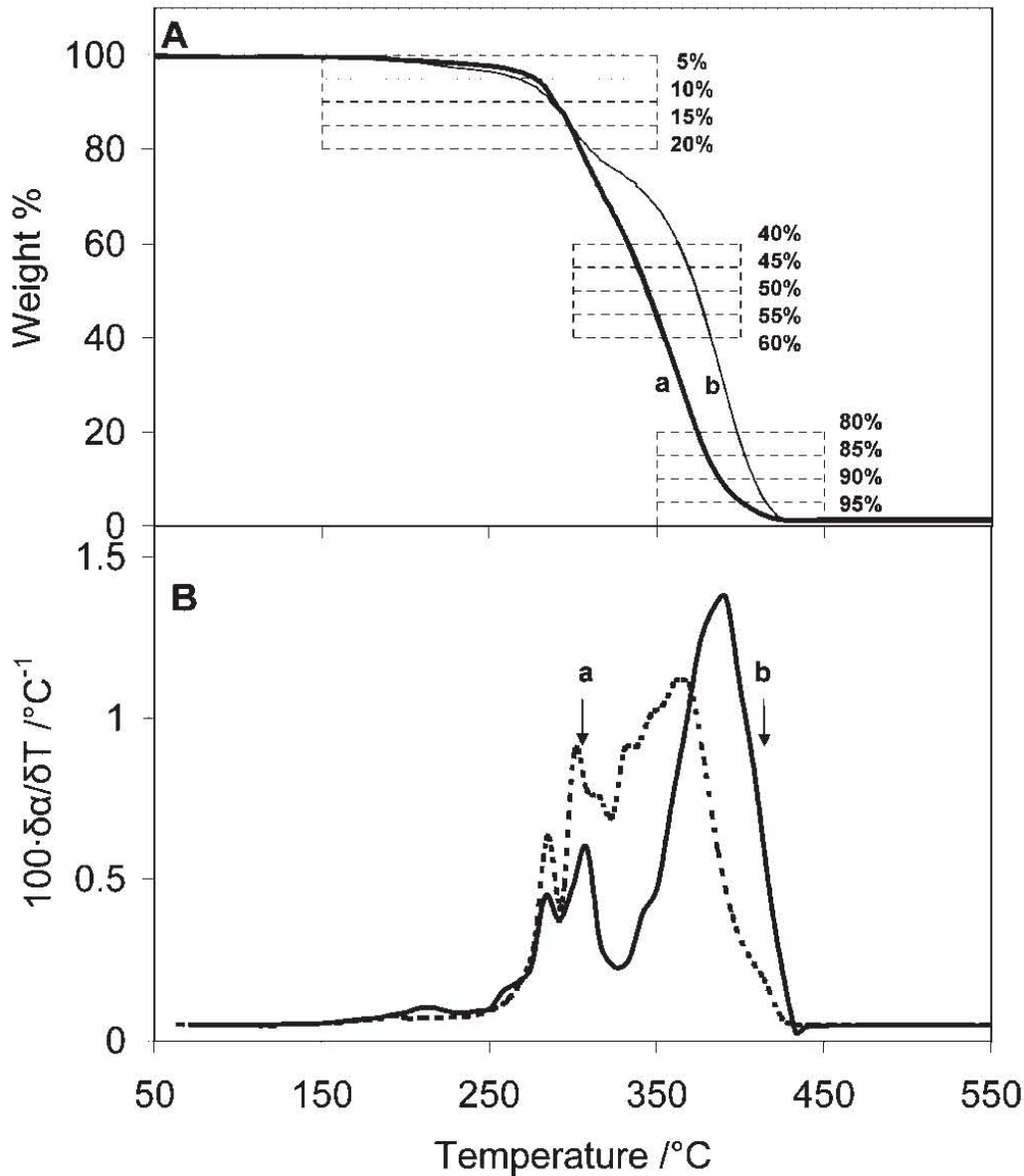
Figure 3

(A) TGA curves for: (a) commercial PMMA (O); (b) PMMA/CHM-0; (c) PMMA/CHM-3 composite.

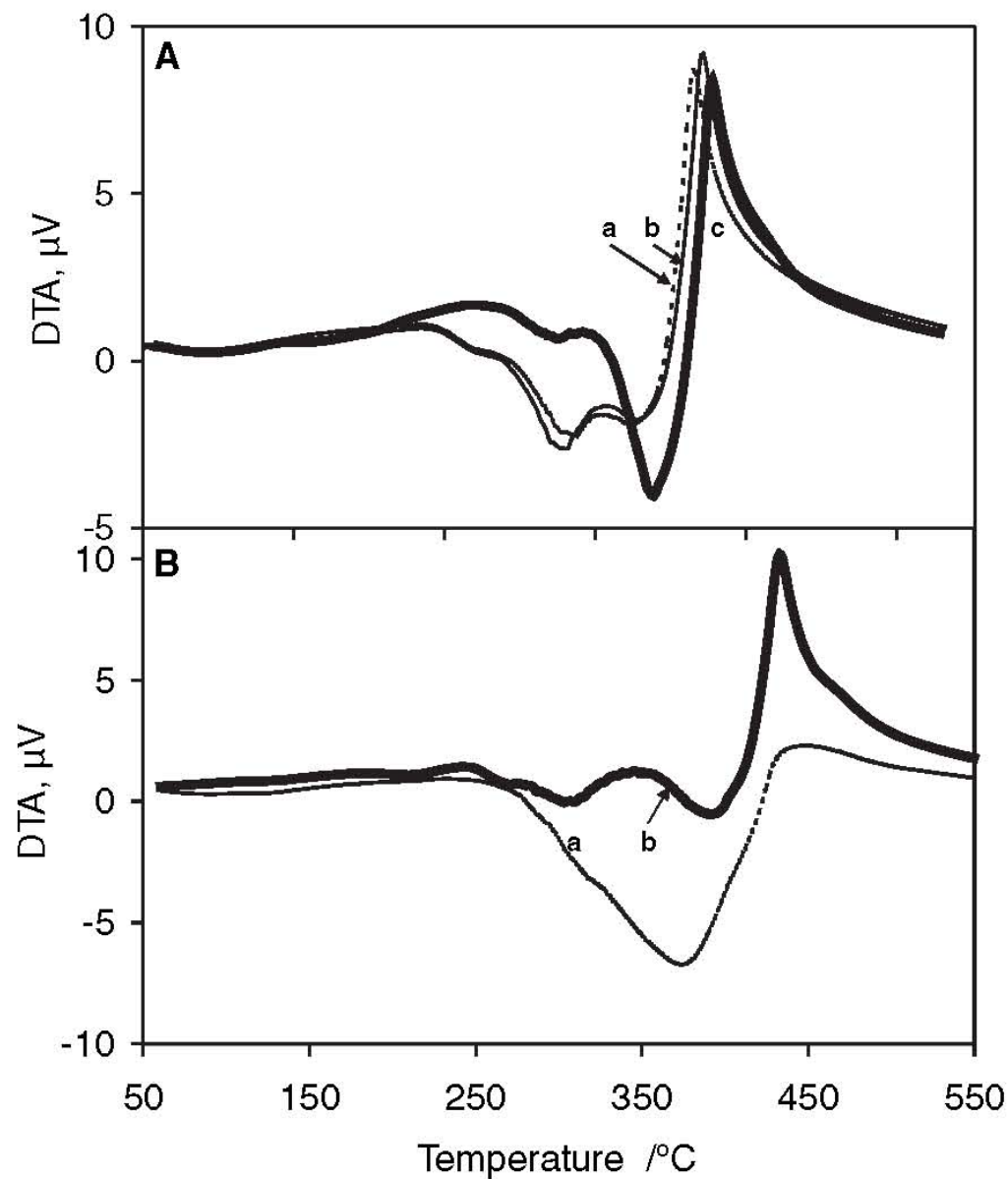(B) DTG curves for: (a) commercial PMMA; (b) PMMA/CHM-0; (c) PMMA/CHM-3 composite.

Figure 4

(A) TGA curves for: (a) pure PMMA; (b) PMMA/CHM-4B synthesized via bulk polymerization.

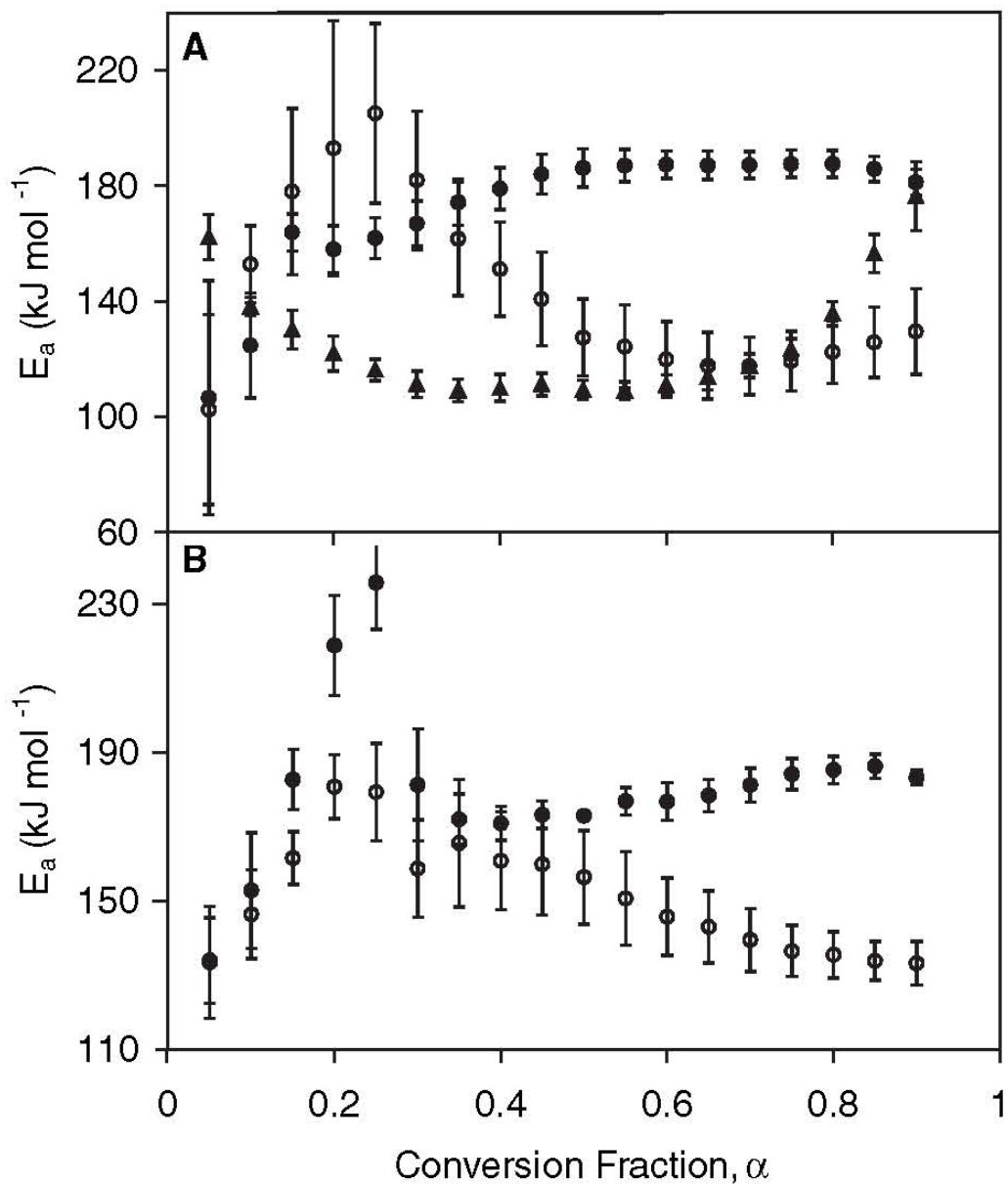(B) DTG curves for: (a) pure PMMA; (b) PMMA/CHM-4B synthesized via bulk polymerization.

Figure 5

(A) TGA curves for: (a) commercial PMMA; (b) PMMA/CHM-0; (c) PMMA/CHM-3 composite.

(B) DTG curves for: (a) pure PMMA; (b) PMMA/CHM-4B synthesized via bulk polymerization.
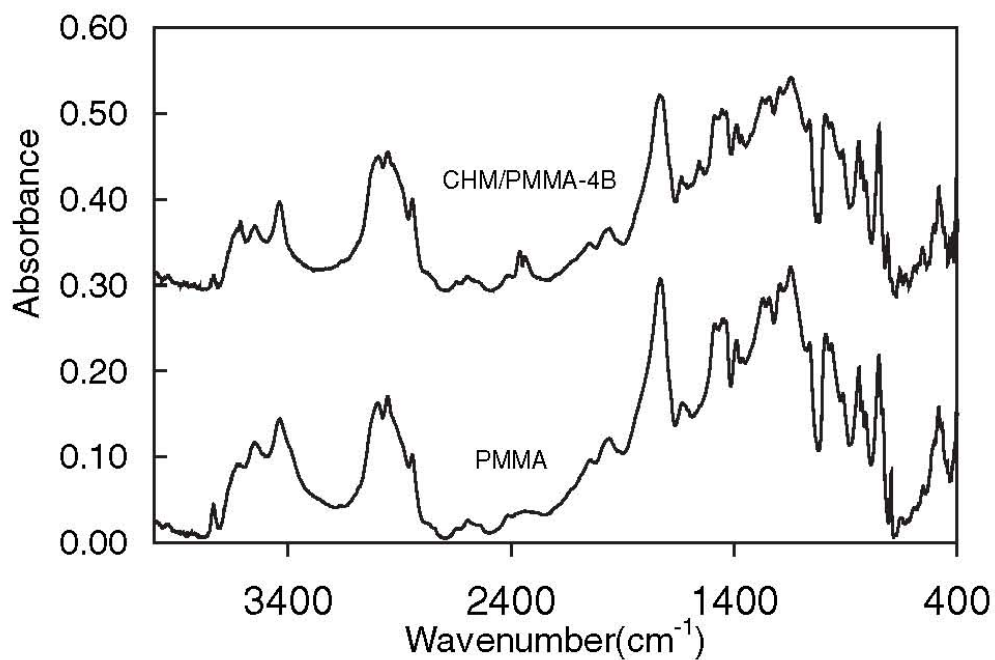
Figure 6

(A) Plot of E_a values versus extent to decomposition, α, for the non-isothermal degradation of commercial PMMA (▲), PMMA/CHM-0 (○), and PMMA/CHM-3 (●).
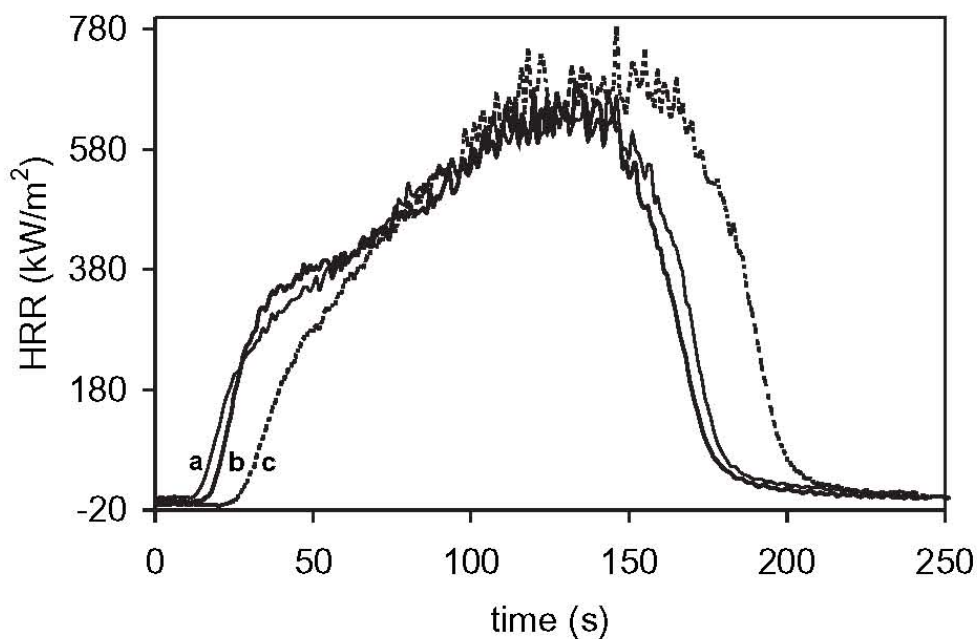
(B) Plot of E_a values α versus for the non-isothermal degradation of pure PMMA (○) and PMMA/CHM-4B (●) synthesized via bulk polymerization.

Figure 7

FT-IR spectra of pure PMMA and PMMA/CHM-4B collected at room temperature. The patterns are offset for clarity but otherwise not scaled.

Figure 8

Heat release rate (HRR) curves for (a) PMMA/CHM-0, (b) PMMA/CHM-3, and (c) commercial PMMA from cone calorimetry measurements at a heat flux of 35 kW m^{-2}.